

ITERATIVE SOLUTION OF MAXWELL'S EQUATIONS FOR AN INDUCTION MOTOR

Shayak Bhattacharjee

Department of Physics,
Indian Institute of Technology Kanpur,
Uttar Pradesh – 208016,
India.

shayak_bhattacharjee@yahoo.co.in

* * * * *

PACS 41.20.-q 41.20.Gz 84.50.+d

ABSTRACT

In this work we use classical electromagnetism to analyse a three-phase induction motor. We first cast the motor as a boundary value problem involving two phenomenological time-constants. These are derived from the widely used equivalent circuit model of the induction motor. We then use an iterative procedure to evaluate these constants and obtain the motor performance equations. Our results depend only on the geometrical parameters of the motor and can be used to derive precise expressions for the excitation frequency and applied voltage needed to extract maximum performance from a given motor at any rotation speed.

* * * * *

INTRODUCTION

Three-phase induction motors play an important role in industry, in the railways and more recently in consumer appliances. This accounts for the considerable contemporary interest in the performance and control of these machines. The standard procedure^{1,2} for analysing the motor is the equivalent circuit method. It is an incisive approach which treats the motor as an electric circuit and computes the voltages and currents in this circuit. However the circuit contains certain parameters (rotor and stator resistances and inductances) which have to be obtained from experiments on the motor and are very difficult or impossible to determine¹ theoretically.

An alternative approach is Finite Element Analysis³⁻⁶ (FEA), a sophisticated numerical algorithm based on physical foundations. The aim of this technique is to cast the motor as a problem in electromagnetism and solve Maxwell's equations for the system by numerical iteration over small volume elements (finite elements). While this algorithm is very precise, it is also very complex and highly specific to each motor. It fails to provide any qualitative physical insight into the working of the motor and the general dependence of the torque on various design parameters. Hence it is not a popular approach in many situations and the equivalent circuit remains the standard model.

A third line of attack⁷⁻⁹ is a cross between a circuit model and an electromagnetic one. Here, the circuit model is used but classical electromagnetism is employed to obtain the parameter values, under certain approximations. This approach is semi-rigorous in that it combines concepts from hardcore electromagnetism, such as Faraday's law, with concepts of a more empirical character, such as magnetomotive forces and flux circuits. The motor is assumed to be two-dimensional in that its height is taken to be infinite. This method is adequate for determining inductances of wound elements but runs into trouble for a cage rotor – bailout is achieved by approximating the rotor bars as wires of negligible cross-sectional area carrying a finite current. In other words the rotor current at any time is modelled as a set of Dirac delta functions at specific angles.

In the present work we aim to develop a formalism which uses purely classical electromagnetism like FEA but is analytic like the equivalent circuit method. The assumptions made by us are more plausible than the ones inherent in the modeling of Refs. 7-9. A recent paper¹² has demonstrated the feasibility of motor analysis using Maxwell's equations as the starting point. That work concerns motors where windings are grouped so that the stator windings of each phase may be treated as point dipoles. Using heavy simplifications, it obtains results which are good at low slips but unsatisfactory at high slips.

In this paper we use an improved model to obtain precise dependences of the output parameters on the inputs and on the geometry of the motor. These will be of use in variable frequency drives^{10,11}. The theoretical nature of our model will come in especially useful while designing application-specific motor/drive combinations where

a priori knowledge of the system's behaviour can lead to conceptualization of the entire design before beginning with implementation.

1. MODELING

Our approach works in the limit that the height of the motor is much larger than the radius, so that the fields may be assumed uniform along the motor axis. Fortunately this is true for many motors as the following pictures (Fig. 1) show.



Figure 1 : Some induction motors where the height far exceeds the radius.

We consider a 2-pole motor, Fig. 2 below.

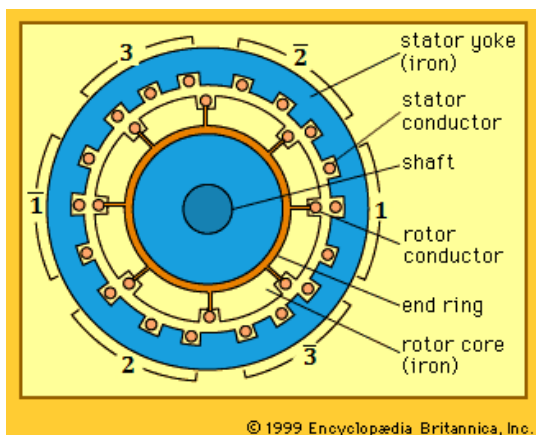


Figure 2 : The 2-pole induction motor, diagram from Ref. 13. Cross-sectional view with the section assumed uniform throughout the entire height. Diagram shows reduced numbers of stator and rotor slots (18 and 8 respectively) to aid understanding. Minor modifications in labelling have been made to conform to the notation used in the text.

We define the height of the motor as h , the radii of the cage and the stator as r and R , the conductivities as σ and σ' and the thicknesses of the conductor as τ and τ' . We treat the rotor and stator as continuous conducting cylinders since the narrow gaps between adjacent bars and wires merely serve to eliminate currents in undesirable directions. The following picture, Fig. 3, of a rotor justifies this assumption.

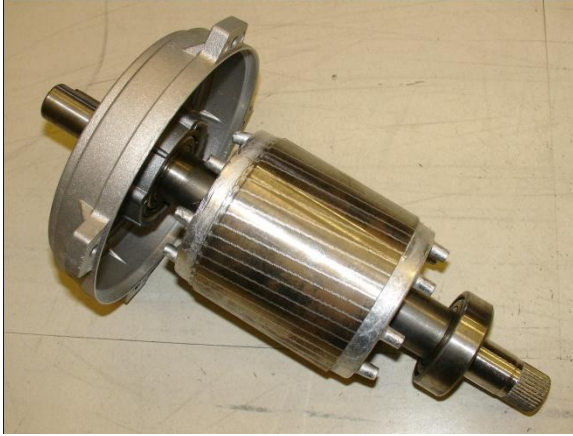


Figure 3 : Closely packed conducting bars on a rotor which can easily be modelled as a continuous cylindrical shell.

Accordingly the final schematic of our model is as below, Fig. 4.

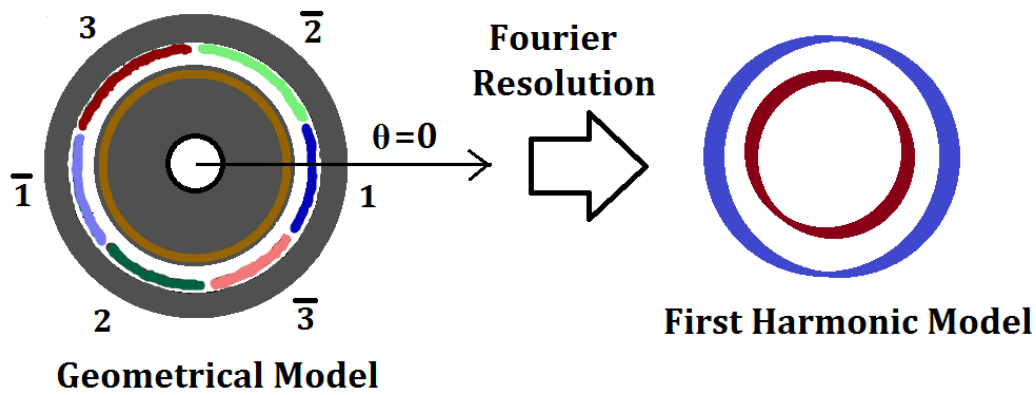


Figure 4 : The left side picture shows the schematic cross-sectional view of our model where the stator and rotor are assumed to be continuous cylindrical shells. The right side picture shows the first angular harmonics of the rotor and stator current, obtained by a Fourier expansion, Eq. (5). The blue band is the stator current and the red the rotor current, the varying thickness being intended to indicate a sinusoidal distribution in space.

The applied stator surface current for the n^{th} phase ($n=1,2,3$) is

$$K_n = K_{\text{app}} \cos(\Omega t + 2(n-1)\pi / 3) \hat{z} \quad (1)$$

in a positive sector (shown in Figs. 2 and 4 as pure numbers) and the negative of that in a negative sector (shown with a bar above the number). Hereafter we assume the \mathbf{z} directionality of the currents to be implicit. Using the angular extensions of the various sectors from Fig. 4, we now expand the applied stator surface current in a Fourier series. The constant term is the sum of the three-phase currents which is zero. The first angular harmonic can be written as

$${}^1K_s = K_{\cos} \cos \theta + K_{\sin} \sin \theta \quad , \quad (2)$$

where K_{\cos} and K_{\sin} are determined the usual way exploiting the completeness and orthogonality of the sines and cosines. We readily obtain

$$K_{\cos} = \frac{1}{\pi} (2K_1 - K_2 - K_3) \quad , \quad (3)$$

and

$$K_{\sin} = -\frac{\sqrt{3}}{\pi} (K_2 + K_3) \quad . \quad (4)$$

Eqs. (3) and (4), show that the $\cos \theta$ component of the stator current leads the $\sin \theta$ component by a quarter cycle in time, whereby the net first harmonic can be written as

$${}^1K_s = K_{\text{app}} \cos(\theta - \Omega t) \quad . \quad (5)$$

This represents a current phasor rotating anticlockwise at frequency Ω . The second and third harmonics vanish due to the symmetries involved in the problem. It is in fact a well-known result that the even and the triplen (multiples of three) harmonics in an induction motor are zero. The derivation of Eq. (5) shows that the n^{th} angular harmonic of the stator current will rotate at a frequency Ω/n . The magnetic field produced by it will also rotate at the same frequency. We note that in the steady state a single rotating magnetic field produces time-independent torque as the profiles of the field at two different times are identical except for a shift through a certain angle, which has no physical significance. The addition of any component at a different frequency destroys this time-invariance and thus leads to fluctuating torque output. This is not desirable so stators are generally designed to eliminate the first few harmonics. Since the n^{th} angular harmonic will have a field contribution at the rotor surface proportional to the $(n-1)^{\text{th}}$ power of (r/R) , the contribution of the still higher harmonics will be negligible anyway.

On this basis we restrict ourselves to analysis of the first angular harmonic only. For a 4-pole motor the first harmonic is $(2\theta \pm \Omega t)$, for a six-pole motor it is $(3\theta \pm \Omega t)$ and so on. We analyse the 2-pole motor here, noting that the technique for the other motors remains the same except for the book-keeping details.

A direct solution of Maxwell's equations is rendered impossible by the fact that we do not know the constitutive relations between the electric fields and the surface currents in the stator and rotor. Our knowledge of the equivalent circuit model convinces us that the stator and rotor are like LR circuits – at present however there is no means of determining the inductances and resistances.

2. ITERATIVE SOLUTION

We now propose the following iterative method¹⁴ for determining the empirical inductances and in the process solving the whole problem. We will first find the current per unit length *applied* to the stator (K_{s0}) and the rotor (K_{r0} , which in this case equals zero) and then find the magnetic field \mathbf{B}_0 created by these currents. Since the tangential component of the magnetic field will not induce any current anywhere, we shall work only with the radial component which we shall denote as \mathbf{B} but without the vector symbol. Subsequently we find the currents induced in the stator (ΔK_{s1}) and rotor (ΔK_{r1}) on account of this magnetic field. Again we calculate the magnetic field ($\Delta \mathbf{B}_1$) due to these induced currents, then again the currents induced by this field, and so on. In this way we generate a sequence of corrections to the basic stator and rotor currents and obtain successive approximations to these quantities by summing all the corrections.

Eq. (5) shows that all currents and magnetic fields will appear stationary in time if we transfer to a frame rotating anticlockwise at frequency Ω ; this is called the synchronous reference frame. Because of this property, all quantities will be evaluated in this frame as functions of the angle θ' alone – the shift to the external frame will result in a replacement of θ' by $\theta - \Omega t$. This special choice of frame is suited for steady-state computations, which shall be our focus in this work.

2A. KNOWN STATOR CURRENT

We first work in the regime that the stator current is given. We temporarily ignore the processes by which the current came about; we just assume that its net value is known. This is physically important as a motor will often operate at the maximum stator current which it can safely tolerate. Constancy of stator current can in fact be achieved by a suitable regulation of the stator voltage – this aspect will be discussed extensively later in this paper. Let the motor rotate counterclockwise and the stator current be

$$K_{\text{stator}} = K_s \sin(\theta - \Omega t) \quad . \quad (6)$$

Then, assuming that the material in the core of the cage is ideal i.e. there are no magnetising dynamics,

$$B_0 = \frac{\mu_{\text{eff}}}{2} K_s \cos(\theta - \Omega t) \quad . \quad (7)$$

Now in the synchronous frame the electric field will be obtained from Faraday's law. But since \mathbf{B} is time-invariant, there will in fact be no electric field in this frame. From the theory of electromagnetic field transformations, there will be an electric field in the rotor frame. This will be obtainable from $\mathbf{E} = -\mathbf{v} \times \mathbf{B}$. We now apply the real Ohm's law i.e. $\mathbf{J} = \sigma \mathbf{E}$ with real conductivity to write the first round of rotor currents as

$$\Delta K_{r1} = \frac{\mu_{\text{eff}}}{2} K_s \sigma r \tau \varepsilon \cos(\theta - \Omega t) \quad . \quad (8)$$

The constant stator current assumption comes in here as B_0 is assumed not to induce any current in the stator. Eq. (8) yields

$$\Delta B_1 = - \left(\frac{\mu_{\text{eff}}}{2} K_s \right) \frac{\mu_{\text{eff}}}{2} \sigma r \tau \varepsilon \sin(\theta - \Omega t) \quad . \quad (9)$$

From this, the general pattern is clear. Successive terms alternate sine with cosine. The following phasor diagram (Fig. 5) clearly shows what is going on.

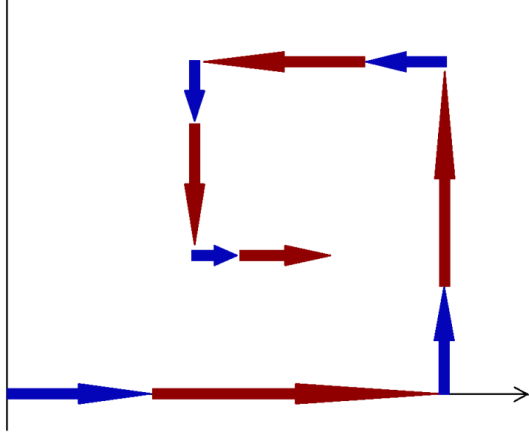


Figure 5 : Phasor diagram showing the rotor currents and the magnetic fields at the rotor surface. The blue phasors are the fields and the red phasors the currents. Each field phasor is shown to induce a corresponding current phasor. Each current phasor produces a new field phasor which leads in phase by 90 degrees.

The cosine terms for the rotor current form a geometric progression with common ratio

$$-\left(\frac{\mu_{\text{eff}}}{2}\sigma_r\tau\varepsilon\right)^2$$

and starting term

$$\frac{\mu_{\text{eff}}}{2}K_s\sigma_r\tau\varepsilon \quad .$$

The sine terms of the rotor current and all the terms of the magnetic field form similar series with different starting terms but the same common ratio. Introducing the substitution

$$\tilde{L} = \frac{1}{2}\mu_{\text{eff}}\sigma_r\tau \quad , \quad (10)$$

we get the net rotor current to be

$$K_r = \frac{K_s\tilde{L}\varepsilon}{1+\tilde{L}^2\varepsilon^2}\left(\cos(\theta-\Omega t)-\tilde{L}\varepsilon\sin(\theta-\Omega t)\right) \quad . \quad (11)$$

The RHS of Eq. (11) is similar to the expression for the current in an inductor hence \tilde{L} is the equivalent of the rotor inductance. This explains the variable definition, Eq. (10). It is somewhat different from the usual definition of inductance as its unit is that of time

unlike the more standard resistance-time. Nevertheless this virtual inductance \tilde{L} captures the basic inductive nature of the rotor circuit. It is of vital importance that the rotor has come out to be an LR circuit as per the experimentally verified predictions of the equivalent circuit model.

The magnetic field at the rotor surface is obtained by dividing the RHS of Eq. (11) by $\sigma\tau\varepsilon$ and is found to be

$$B_r = \frac{\mu_{\text{eff}}}{2} \frac{K_s}{1 + \tilde{L}^2 \varepsilon^2} \left(\cos(\theta - \Omega t) - \tilde{L} \varepsilon \sin(\theta - \Omega t) \right) . \quad (12)$$

To find the torque we convert the K to an I by multiplying by the infinitesimal length element $r d\theta$, multiply an h to account for the length of current flow and an r to convert force to torque, and integrate over the whole cage, getting

$$\Gamma = r^2 h \int_0^{2\pi} \left(K_r \right)_{t=0} \left(B_r \right)_{t=0} d\theta , \quad (13)$$

in which we have used the time independence of torque discussed after Eq. (5).

From Eqs. (11), (12) and (13), the torque is

$$\Gamma = \frac{\pi}{2} \mu_{\text{eff}} K_s^2 r^2 h \frac{\tilde{L} \varepsilon}{1 + \tilde{L}^2 \varepsilon^2} . \quad (14)$$

While working with conductivities and permeabilities we note that for a sinusoidal current or field, their values may depend on the frequency. In conductors, the skin effect reduces the conductivity at high frequencies, in ferromagnets, hysteresis may diminish the field amplitudes. Since in the 2-pole motor the rotor electrical frequency is ε , conductivity should properly be written as $\sigma(\tau, \varepsilon)$ and permeability as $\mu_{\text{eff}}(\varepsilon)$. To determine these functions, experiments on the materials will have to be carried out. These experiments however must not be confused with the experiments on actual motors which are required for parameter determination in an equivalent circuit.

As an exercise in comparing our results with the standard formulae, we try to estimate the rotor parameters of the 2-pole motor in Problem 7.14, Ref. 1. The exact values of μ_{eff} , σ , r and τ are difficult or impossible to obtain without performing a destructive test on the motor, so we resort to estimating these parameters. The motor is given to be of 75 kW rating which implies an IEC frame size of 280. The external stator radius for this is 14 cm and we can assume a rotor radius of about half that i.e. 7cm. The rotor currents typically reach maximum values of about 300 A and the rotors are generally made of aluminium with dc conductivity 3×10^7 Siemen. It can be determined from any gauge

calculator that the conductor must have a thickness of approximately 3 mm to tolerate this current level. The rotor core is typically made of mild steel with laminations and the permeability may be assumed as $100\mu_0$. Under these conditions,

$$\tilde{L} = \frac{1}{2} \times (10^{-4}) \times (3 \times 10^7) \times (7 \times 10^{-2}) \times (3 \times 10^{-3}) \quad ,$$

where each pair of parentheses encloses the value in SI units of the corresponding parameters in Eq. (10). This expression evaluates to approximately 0.3 s, in good agreement with the value of 0.2 s obtained by working out the exercise. Moreover our values have come out on the higher side, which is expected as the frequency effects mentioned after Eq. (14) will all tend to reduce the time constant. Below in Fig. 6 we show a torque speed plot obtained from Eq. (14) (in red) superposed on a torque-speed characteristic (black) from Ref. 10. As this was drawn for an arbitrary motor with unspecified parameters, we choose our parameters so that the maximum of our curve corresponds to the maximum of the reference curve. We see that a close match occurs not just at the maximum but across the entire operating range. Thus our torque-speed characteristics are very nearly identical to those obtained from the equivalent circuit method.

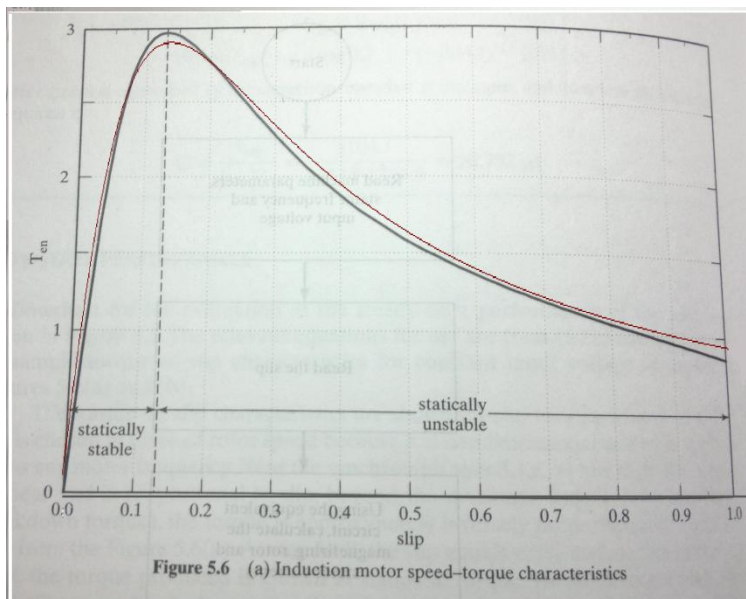


Figure 6 : Image of Fig. 5.6, Ref. 10. Slip is along the x axis and torque along the y axis. Superposed on it in red is the curve corresponding to Eq. (14) with the parameters extrapolated from the original graph. The comparison shows that both the graphs have the same dependence on the slip.

This graph also resolves a technical detail regarding Eqs. (11) to (13), which are strictly valid only when $\tilde{L} < 1$ as the geometric series can be summed only under this condition. Nevertheless, their RHS'es do not diverge even when this condition is not satisfied and

we claim that they are valid outside of this range too. We see that $\tilde{L}\varepsilon = 1$ at the maximum point on the graph and our claim is verified since our formula continues to give accurate results beyond that point.

We now focus on how to determine the stator current. The stator parameters must be computed from a formalism similar to that employed for the rotor. As mentioned in the discussion following Eq. (5) we shall neglect higher angular harmonics and assume the stator to carry currents of the form $K \cos(\theta - \Omega t + \varphi)$. The voltage applied to the stator manifests itself as the *applied* stator current which we take without loss of generality as

$$K_{s0} = K_0 \cos(\theta - \Omega t) \quad . \quad (15)$$

The applied stator current amplitude K_0 is of course *directly proportional* to the applied voltage so in future we may use K_0 itself to refer to the applied stator voltage. Magnetic fields and induced currents are as in the rotor. We assume for the time being that the rotor does not have any effect on the stator – all stator magnetic fields and currents are due to the stator alone. This is the independent stator approximation and is valid if (a) the stator surface currents are much larger than their rotor counterparts and (b) r/R is small. It is worth studying due to the simplicity of the calculations involved; the general case where the stator and rotor mutually influence each other is left for the next section and is considerably more laborious.

Analogous to the rotor, we define the virtual stator inductance as

$$\tilde{M} = \frac{1}{2} \mu_{\text{eff}} \sigma' R \tau' \quad . \quad (16)$$

Comparing K_{s0} with ΔK_{r1} in Eq. (8) and carrying through the formalism yields

$$K_{\text{stator}} = \frac{K_0}{1 + \tilde{M}^2 \Omega^2} \left(\cos(\theta - \Omega t) - \tilde{M} \Omega \sin(\theta - \Omega t) \right) \quad . \quad (17)$$

The phase of this current relative to K_{s0} is unimportant as it is of no physical significance. What matters is its amplitude which is

$$K_s = \frac{K_0}{(1 + \tilde{M}^2 \Omega^2)^{1/2}} \quad . \quad (18)$$

Eq. (18) will come in useful while determining the voltage amplitude to be applied to the stator to ensure that the stator current remains constant. This mode will be useful when the maximum permissible stator current is the limiting factor in the motor

performance. Eq. (18) indicates that to maintain stator current constant, the voltage must be increased as Ω increases; this relationship is the basis for the constant volts/Hz control scheme. Above a certain Ω , the voltage requirement will tend to exceed the capabilities of the inverter. The maximum inverter voltage will then become the limiting factor and the motor will enter the flux weakening^{10,15,16} regime. Now, Eq. (18) will yield the stator current in terms of the constant K_0 and this value must be plugged into Eq. (14) to obtain the torque. Writing $\Omega=\omega+\varepsilon$ in the torque equation thus found and differentiating it with respect to ε will yield the value of slip frequency needed to produce maximum torque output at every value of rotor speed.

We now proceed to the case where the independent stator approximation is not applicable.

2B. KNOWN STATOR VOLTAGE

The calculation in this section is similar to that in Sec. 2A but this time the effect of the rotor on the stator will be taken into account. A marginal calculational convenience occurs if we assume the first angular harmonic of the applied (zeroth order) stator current to be a sine instead of a cosine, as we had taken in Eq. (15) to directly exploit the analogy with Eq. (8). Accordingly, we set

$$K_{s0} = K_0 \sin(\theta - \Omega t) \tag{19}$$

and the applied rotor current is of course zero. B_0 is as in Sec. 2A but this time it induces ΔK_{r1} in the rotor and ΔK_{s1} in the stator. These two together contribute to ΔB_1 which again induces currents in both the stator and the rotor. The development appears complicated but can be resolved by separately considering the effect of each stator and rotor current phasor, Fig. 7 below.

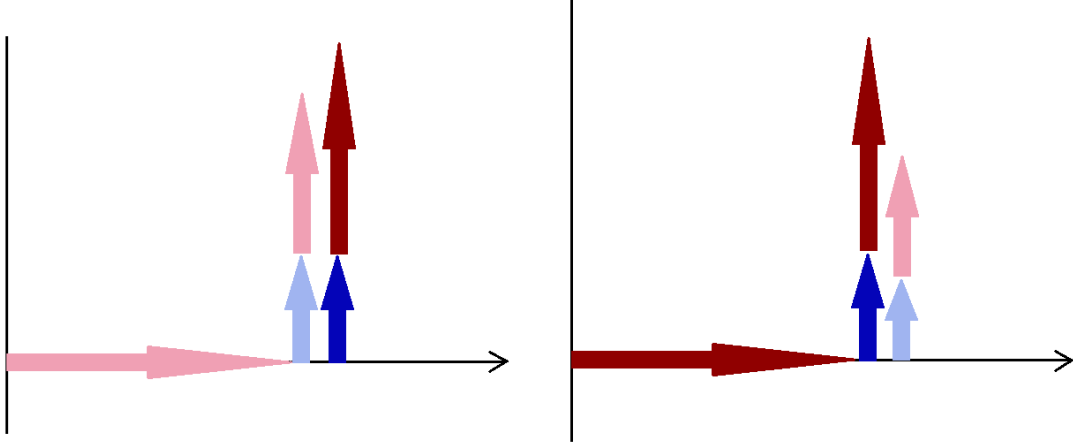


Figure 7 : Current phasors in red shades and field phasors in blue. Light colours used for the stator and dark colours for the rotor. The diagram on the left shows a stator current phasor and its offshoots. The diagram on the right shows the same for a rotor current phasor.

Every stator current phasor produces the same magnetic field at the surface of the stator and the rotor; the magnitude conversion factor is $\mu_{\text{eff}}/2$ and the field leads the current in phase by 90 degrees. This magnetic field induces currents in the stator and the rotor, the former with magnitude converter $\sigma'R\tau\Omega$ and the latter with converter $\sigma\tau\epsilon$. Each rotor current phasor induces magnetic fields at the stator and rotor surfaces – the former with magnitude converter $\frac{\mu_{\text{eff}}}{2} \frac{r^2}{R^2}$ and the latter with converter $\mu_{\text{eff}}/2$. These induce currents in their respective elements with the same magnitude converters as mentioned previously.

Temporarily using complex notation, the relations described here can be expressed in terms of a transformation matrix \mathbf{T} , as follows.

$$\begin{bmatrix} \Delta K_{r(n+1)} \\ \Delta K_{s(n+1)} \end{bmatrix} = i \frac{\mu_{\text{eff}}}{2} \begin{bmatrix} \sigma\tau\epsilon & \sigma\tau\epsilon \\ \frac{r^2}{R^2} \sigma'R\tau\Omega & \sigma'R\tau\Omega \end{bmatrix} \begin{bmatrix} \Delta K_{rn} \\ \Delta K_{sn} \end{bmatrix} \quad . \quad (20)$$

Here the phasors in the two column vectors must be represented in complex exponential form. A change of variables expresses this matrix as

$$\mathbf{T} = i \begin{bmatrix} C_r & C_r \\ \frac{r^2}{R^2} C_s & C_s \end{bmatrix} = i C_r \begin{bmatrix} 1 & 1 \\ \eta & \varsigma \end{bmatrix} \quad . \quad (21)$$

Now the n^{th} order phasors are given by

$$\begin{bmatrix} \Delta K_{rn} \\ \Delta K_{sn} \end{bmatrix} = T^n \begin{bmatrix} 0 \\ K_0 \exp i(\theta - \Omega t - \pi / 2) \end{bmatrix} \quad (22)$$

where we have written the applied rotor and stator currents in the vector on the RHS.

A glance at Eqs. (20) and (22) or at Fig. 7 convinces us that alternate terms will be sines and cosines so we discard the exponential notation at this stage and directly work with real quantities. The k^{th} order sine terms will be given by

$$\begin{bmatrix} \Delta K_{rk\sin} \\ \Delta K_{sk\sin} \end{bmatrix} = T^{2(k-1)} \begin{bmatrix} 0 \\ K_0 \sin(\theta - \Omega t) \end{bmatrix} . \quad (23)$$

Likewise the k^{th} order cosine terms will be given by

$$\begin{bmatrix} \Delta K_{rk\cos} \\ \Delta K_{sk\cos} \end{bmatrix} = T^{2(k-1)} \begin{bmatrix} C_r K_0 \cos(\theta - \Omega t) \\ C_s K_0 \cos(\theta - \Omega t) \end{bmatrix} \quad (24)$$

where the vector on the RHS has been derived by substituting $n=1$ in Eq. (22).

Another change of variables is carried out as per the following equation.

$$T^2 = -C_r^2 \begin{bmatrix} 1+\eta & 1+\zeta \\ \eta(1+\zeta) & \eta+\zeta^2 \end{bmatrix} = -C_r^2 \begin{bmatrix} W & X \\ Y & Z \end{bmatrix} . \quad (25)$$

The eigenvalues of T^2 are

$$\lambda_1 = \frac{1}{2} \left(W + Z + \sqrt{(W - Z)^2 + 4XY} \right) \quad (26)$$

and

$$\lambda_2 = \frac{1}{2} \left(W + Z - \sqrt{(W - Z)^2 + 4XY} \right) \quad . \quad (27)$$

The eigenvectors corresponding to the two values are $\begin{bmatrix} X \\ \lambda_1 - W \end{bmatrix}$ and $\begin{bmatrix} X \\ \lambda_2 - W \end{bmatrix}$

respectively. This yields

$$T^{2k} = \frac{1}{X(\lambda_2 - \lambda_1)} \begin{bmatrix} \lambda_2 - W & W - \lambda_1 \\ -X & X \end{bmatrix} \begin{bmatrix} \lambda_1^k & 0 \\ 0 & \lambda_2^k \end{bmatrix} \begin{bmatrix} X & X \\ \lambda_1 - W & \lambda_2 - W \end{bmatrix} \quad . \quad (28)$$

We will not show the subsequent steps of solving Eqs. (23) and (24) explicitly but proceed directly to the results after carrying out the summations over k. We have

$$\begin{aligned} K_{\text{stator}} &= K_0 \left(\frac{1}{\lambda_2 - \lambda_1} \left(\frac{X}{1 + C_r^2 \lambda_1} - \frac{(\lambda_2 - W)}{1 + C_r^2 \lambda_2} \right) \right) \sin(\theta - \Omega t) \\ &+ \frac{K_0}{\lambda_2 - \lambda_1} \left(\frac{X(C_r + C_s)}{1 + C_r^2 \lambda_1} - \frac{(\lambda_1 + \lambda_2 - 2W)}{1 + C_r^2 \lambda_2} \right) \cos(\theta - \Omega t) \end{aligned} \quad . \quad (29)$$

Likewise

$$\begin{aligned} K_{\text{rotor}} &= \frac{K_0(W - \lambda_2)}{\lambda_2 - \lambda_1} \left(\frac{1}{1 + C_r^2 \lambda_1} + \frac{(W - \lambda_1)}{X(1 + C_r^2 \lambda_2)} \right) \sin(\theta - \Omega t) \\ &+ \frac{K_0}{\lambda_2 - \lambda_1} \left(\frac{(W - \lambda_2)(C_r + C_s)}{1 + C_r^2 \lambda_1} + \frac{C_r(W - \lambda_1)^2 + C_s(W - \lambda_1)(W - \lambda_2)}{X(1 + C_r^2 \lambda_2)} \right) \cos(\theta - \Omega t) \end{aligned} \quad . \quad (30)$$

These functions are rather complex so we plot graphs of the K's vs. ε and Ω as Figs. 8a and 8b below.

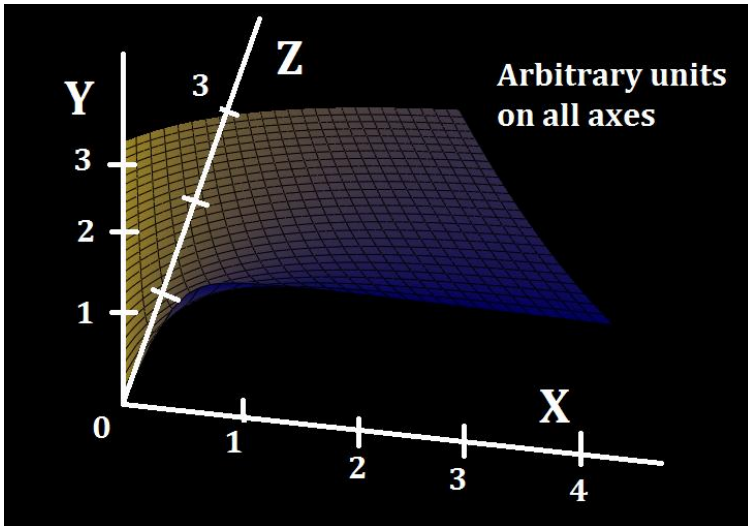


Figure 8a : Magnitude of rotor current (z axis) vs. slip frequency (x axis) and excitation frequency (y axis). Colour is dependent on elevation.

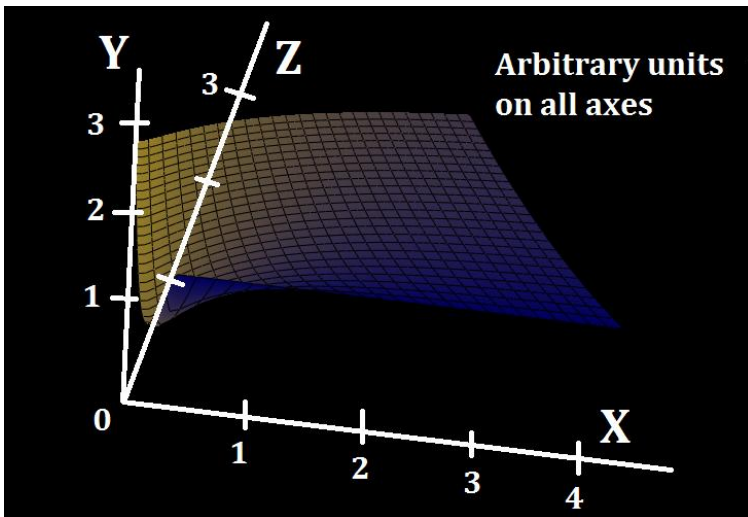


Figure 8b : Magnitude of stator current (z) vs. slip frequency (x) and excitation frequency (y) at constant stator voltage. In both these plots, the relevant region is bounded by the plane $y=x$, for the slip frequency cannot exceed the excitation frequency.

We make a brief note regarding the higher angular harmonics discussed after Eq. (5). Though we have neglected these harmonics, their analysis can be carried out in a style identical to that used for the first harmonic. Infinite order perturbation in the appropriate synchronous frame will yield expressions for the field and current due to each harmonic; subsequently the resultants are to be added to form expressions for the net field and current. An integration similar to that in Eq. (13) but with the $t=0$ values replaced by time dependent expressions yields the torque, which of course fluctuates with time. As has already been mentioned, the procedure for analysing these higher harmonics of the 2-pole motor is identical to that for treating the principal harmonics of 4, 6 or higher pole motors.

CONCLUSION

Application of classical electromagnetic theory to the induction motor has proved to be a very profitable exercise. The results obtained from our application of infinite-order perturbation theory are in good agreement with experiments and with the existing literature. Our formulae are of considerable utility at various levels. Eqs. (12), (13) and (14) in the independent stator approximation and their equivalents in the coupled element regime will enable prediction of the performance of a motor from knowledge of its geometry. These relations will be especially useful to motor designers. Moreover our work provides very precise relations between the input and output parameters. These relations will be important in the field of motor control using variable frequency drives, which are a topic of considerable contemporary interest on account of their ubiquity.

* * * * *

ACKNOWLEDGEMENT

I would like to thank Prof. Jayanta K. Bhattacharjee for valuable discussion. I am also grateful to KVPY, Govt. of India for a fellowship.

REFERENCES

1. S. J. Chapman, "*Electric machinery fundamentals*," Fourth ed. Mc Graw Hill, New York, USA (2005)
2. V. del Toro, "*Electrical engineering fundamentals*," Prentice Hall, New Jersey, USA (1972)
3. M. S. Sarma, "Generalised prediction model of the induction motor," J. Appl. Phys. **57**, 3878 (1985)
4. E. Vassent, G. Meunier, A. Foggia and G. Reyne, "Simulation of induction machine operation using a step by step finite element method coupled with circuits and mechanical equations," IEEE Trans. on Magnetics **27** (6), 5232-5234 (1991)
5. L. Alberti, N. Bianchi and S. Bolognani, "Field oriented control of induction motor: a direct analysis using finite element," IECON 2008 34th annual Conference of IEEE, 1206-1209 (2008)

6. C. A. da Silva, F. Bidaud, P. Herbet and J. R. Cardoso, "Power factor calculation by the finite element method," *IEEE Trans. on Magnetics* **46** (8), 3002-3005 (2010)
7. J.L. Kirtley, "6.685 *Electric Machines*," Massachusetts Institute of Technology : MIT OpenCourseWare (2005)
8. A. E. Fitzgerald, C. Kingsley and S. D. Umans, "*Electric machinery*," Sixth ed. Tata McGraw-Hill, New Delhi (2009)
9. P. L. Alger, "*Induction Machines : Their Behavior and Uses*," Taylor and Francis, New York, USA (1995)
10. R. Krishnan, "*Electric motor drives – modeling, analysis and control*," PHI Learning Private Ltd. New Delhi, India (2010)
11. R. J. Kerkman, G. L. Skibinski and D. W. Schlegel, "AC Drives: year 2000 (Y2K) and beyond," 14th Annual Applied Power Electronics Conference and Exposition **1**, 28-39 (1999)
12. S. Bhattacharjee, "Analysis of a three-phase induction motor directly from Maxwell's equations," *Am. J. Phys.* **80** (1), 43-46 (2012)
13. "*Electric Motor*," Encyclopaedia Britannica : Encyclopaedia Britannica Online Academic Edition (2012)
14. T. Roy, S. Ghosh and J. K. Bhattacharjee, "Perturbation theory for Maxwell's equations with a time-dependent current source," *EPJ Plus* **126** (12), 119 (2011)
15. F. Briz, A. Diez, M. W. Degner and R. D. Lorenz, "Current and flux regulation in field weakening operation of induction motors," *IEEE Trans. on Ind. Appl.* **37** (1), 42-50 (2001)
16. M. Mengioni, L. Zarri, A. Tani, G. Serra and D. Casadei, "Stator flux vector control of induction motor drive in the field weakening region," *IEEE Trans. on Power Elec.* **23** (2), 941-949 (2008)